THE ASTROPHYSICAL JOURNAL, 253:908–920, 1982 February 15

A NEW TEST OF GENERAL RELATIVITY: GRAVITATIONAL RADIATION AND THE BINARY PULSAR PSR 1913+16

J. H. TAYLOR AND J. M. WEISBERG
Department of Physics and Astronomy, University of Massachusetts, Amherst; and Joseph Henry Laboratories, Physics Department, Princeton University
Received 1981 July 2; accepted 1981 August 28

ABSTRACT

Observations of pulse arrival times from the binary pulsar PSR 1913+16 between 1974 September and 1981 March are now sufficient to yield a solution for the component masses and the absolute size of the orbit. We find the total mass to be almost equally distributed between the pulsar and its unseen companion, with $m_p = 1.42 \pm 0.06\ M_\odot$ and $m_c = 1.41 \pm 0.06\ M_\odot$. These values are used, together with the well determined orbital period and eccentricity, to calculate the rate at which the orbital period should decay as energy is lost from the system via gravitational radiation. According to the general relativistic quadrupole formula, one should expect for the PSR 1913+16 system an orbital period derivative $\dot{P}_b = (-2.403 \pm 0.005) \times 10^{-12}$. Our observations yield the measured value $\dot{P}_b = (-2.30 \pm 0.22) \times 10^{-12}$. The excellent agreement provides compelling evidence for the existence of gravitational radiation, as well as a new and profound confirmation of the general theory of relativity.

Subject headings: gravitation — pulsars — relativity

I. INTRODUCTION

The orbiting pulsar PSR 1913+16 discovered by Hulse and Taylor (1975*a*) has now been observed for more than 6 years. This pulsar, as an accurate clock moving at high velocity in the strong gravitational field of its unseen companion, offers an unprecedented opportunity for tests of the nature of gravitation. Progress reports summarizing the available data and observing methods have been published several times during the 6 year interval (Taylor *et al.* 1976; Fowler, Cordes, and Taylor 1979; McCulloch, Taylor, and Weisberg 1979; Weisberg and Taylor 1981), including an announcement of the detection of changes in the orbital period at a rate consistent with gravitational radiation damping (Taylor, Fowler, and McCulloch 1979). In the present paper we describe all of the existing observations through 1981 March in greater detail (§ II), and we give particulars on our method of analyzing the data (§ III). The results of this analysis, which represent our current level of understanding of the dynamics of the orbiting system, are presented in § IV. Finally, in § V we argue that the observed rate of decay of the orbit firmly establishes the existence of gravitational radiation as predicted by general relativity. At the same time, several other theories of gravity are shown to be inconsistent with the observations. The nature of the unidentified companion star, and its possible effect upon our conclusions, are discussed in Appendix A. Some new observational data on PSR 1913+16, only indirectly related to the timing measurements, are presented in Appendix B.

II. OBSERVATIONS FROM 1974.8 TO 1981.2

a) Evolution of the Data Acquisition System

PSR 1913+16 is a pulsar of unusually short period, $P = 0.059$ s, moving in a binary orbit of period $P_b = 7^h45^m$ and eccentricity $e = 0.617$. Its flux density at 430 MHz is approximately 5 mJy, which makes it one of the weakest known pulsars. A large dispersion measure (DM = 168.77 cm^{-3} pc) also conspires to make observations difficult: without some kind of dispersion-compensating hardware, the differential time delay across a typical bandwidth of 4 MHz at 430 MHz would be 70 ms, or considerably more than the pulsar period, and the pulsar would be unobservable.

All of our data have been taken at frequencies near 430 MHz or 1410 MHz, using the 305 m telescope at the Arecibo Observatory.[1] The early observations of this pulsar, including its initial discovery, were made with equipment explicitly designed to optimize the detectability of dispersed, periodic signals (Hulse and Taylor 1974, 1975*b*; Hulse 1975). This equipment operated at 430 MHz and made use of a dual 32×250 kHz filter bank to allow postdetection dispersion removal. The available time resolution with this system is ultimately limited by the dispersive delay across a single 250 kHz channel, approximately 4.4 ms for PSR 1913+16.

The basic observations of relevance to this paper are measurements of arrival times of the pulses. As is true

[1]The Arecibo Observatory is part of the National Astronomy and Ionosphere Center, which is operated by Cornell University under contract with the National Science Foundation.

TABLE 1

PARAMETERS OF OBSERVING SYSTEMS USED FOR PSR 1913+16

Dates	Frequency (MHz)	Total Bandwidth (MHz)	Frequency Channels	Number of Polarizations	System Noise Temp. (K)	Recording Method[a]	Time Resolution (μs)	RMS Measurement Uncertainty (μs)	Number of Observations	Nominal Assigned Weight
A. 1974 Sep–Dec	430	8.0	32	2	175	FS	5000	275	524	0.04
B. 1975 Apr–1976 Nov	430	0.64 or 3.2	32	1 or 2	175	AVG	2000	310	112	0.01
C. 1975 Jun–1976 Feb	430	0.25	1	2	175	AVG	2000	890	75	0.001
D. 1976 Nov–Dec	430	0.64	32	1	175	FS	750	155	73	0.1
E. 1977 Jul–Aug	430	0.64	32	1	175	AVG	340	150	52	0.1
F. 1978 Jun–1981 Feb	430	3.34	504	2	175	AVG	43	75	572	1.0
G. 1977 Jul–Aug	1410	8.0	32	2	80	AVG	125	75	57	0.2
H. 1977 Dec	1410	8.0	32	2	80	AVG	125	55	45	0.6
I. 1978 Mar–Apr	1410	8.0	32	2	80	FS	125	50	120	1.0
J. 1980 Jul–1981 Feb	1410	8.0	32	2	80, 40	AVG	200	85	312	1.0
K. 1981 Feb–Mar	1410	16.0	64	2	40	AVG	125	25	415	2.0

[a]FS means fast-sampled raw data were recorded on magnetic tape, with timing information; AVG means synchronous signal averaging was done at the time of observation, using a precomputed ephemeris.

for other pulsars, accurate timing observations require both good time resolution and high signal-to-noise ratio (S/N), and these requirements place conflicting demands on receiver bandwidth. Furthermore, PSR 1913+16 is much too weak to permit the observations of individual pulses, so synchronous averaging must be used—typically over periods of several minutes or longer. As in the case of bandwidth, a compromise must be made by choosing an integration time large enough to provide good S/N, yet not more than a small fraction of the orbital period.

For these reasons, we have directed considerable effort toward developing receiving techniques which improve the time resolution while maintaining high S/N in approximately 5 minutes of integration. Some results of this work are summarized in Table 1, which lists the relevant attributes and statistics of 11 different data acquisition systems used for PSR 1913+16 (labeled A through K). All of the systems except C and F made use of 32 channel postdetection de-dispersers of analog (A, B, K; Taylor and Huguenin 1971) and/or digital circuitry (B, D, E, G–K; Boriakoff 1973). System F, used between 1978 June and 1981 February, has been described in detail elsewhere (McCulloch, Taylor, and Weisberg 1979). It uses a swept-frequency technique and a digital autocorrelator to remove most of the effects of dispersion before detection, and in principle achieves the best time resolution of any of our observing systems, about 43 μs.

Most of the observations made with system B, and all of C, were made as part of a general program of pulsar timing observations (Gullahorn and Rankin 1978; Taylor *et al.* 1976), and for this reason the parameters were not optimized for the binary pulsar. With these exceptions, however, the results obtained with all of the 430 MHz receiving systems have improved steadily since 1974. As shown in Figure 1, the time resolution at 430 MHz has been improved from 5000 μs (with receiving system A) to the present 43 μs. Because part of this improvement comes at the expense of reduced S/N, and because the narrowest features of the pulse are now well resolved, the improvement in timing accuracy at 430 MHz is a smaller (but still impressive) factor of about 4, from 275 μs to 75 μs.

Since 1977, much of our observing has been done at frequencies near 1410 MHz instead of 430 MHz. Although the pulsar has a very steep spectrum, with a mean flux density of only about 1 mJy at 1410 MHz, the lower galactic background temperature and larger bandwidth usable at the higher frequency compensate almost fully. Also, as shown in Figure 1, the pulse profile at 1410 MHz lacks the central component and has somewhat steeper edges—which is an aid to timing measurements. These factors combine to make most of the 1410 MHz timing data better in quality than the best 430 MHz data. The most recent observations (1981 February–March: system K in Table 1) were aided by a new cooled field effect transistor (FET) preamplifier and twice the bandwidth of previous observations. The rms measurement uncertainty for 5 minute integrations with system K was about 25 μs.

As indicated in Table 1, some of the data (those from systems A, D, and I) were recorded in raw form, by digitizing the receiver output at rates as high as 10 kHz and storing the numbers on magnetic tape, together with appropriate timing information. Subsequent analysis required "folding" the data modulo the apparent pulsar period, in blocks about 5 minutes (or 5000 pulsar periods) long, to form average pulse profiles. For the remaining observations, the synchronous averaging was

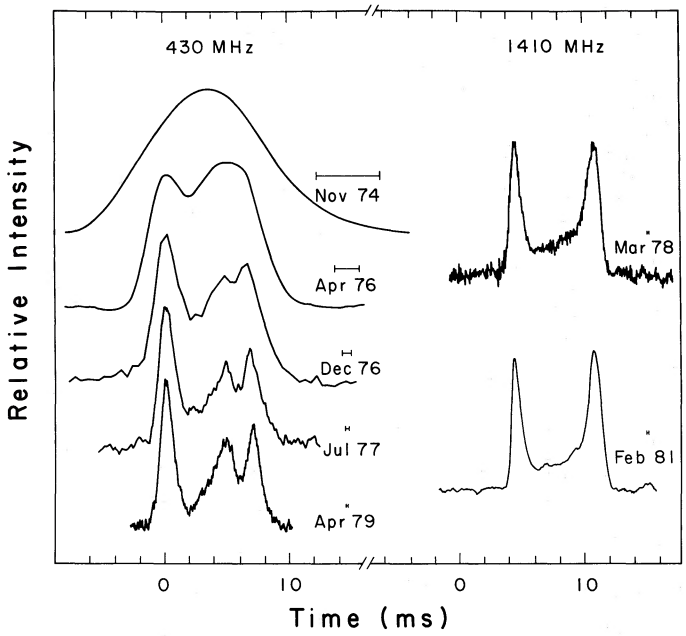

FIG. 1.—Average pulse profiles obtained for PSR 1913+16 over the period 1974–1981, at 430 MHz and 1410 MHz. The changes in shape are the result of improved dispersion removal techniques and consequent improvements in time resolution, as indicated by the horizontal bars.

done in real time, so that average profiles could be viewed immediately, and equipment performance verified. On-line averaging has many advantages, but requires that the pulsar period be predictable at all times to an accuracy of ~1 ns or better, and that the oscillator used to synchronize the signal averaging with the apparent pulse period be updated at least once every few seconds. These criteria have been met for all observations taken since late 1977. Because most of the early data (systems A and D) were recorded in raw form, it was possible to refold them after more accurate ephemeris parameters had been obtained, so they also meet the criteria for accurately synchronized signal averaging. The data from systems B and C could not be so treated *a posteriori*, and (as described in § III) are known to contain some systematic errors because of pulse smearing during the averaging process. These data have been assigned reduced weights in the final analysis.

b) Determination of Pulse Arrival Times

The basic data from which we estimate the pulse arrival times consist of average pulse profiles, usually 1024 bins in length, representing about 5 minutes of data acquisition. The Coordinated Universal Time of the first phase bin of the pulse profile (as measured near the middle of the 5-minute integration) is also available, having been recorded (to an accuracy of ~1 μs) at the time of observation. The average profiles shown in Figure 1 were made by summing nearly all of the available 5 minute averages for a given observing system, taking care to align them as accurately as possible. The sum was then used as a standard profile, or template, against which the phase of each individual profile could be measured by a least squares fitting technique. The measured phases, together with the time of the first bin, give an "arrival time" for a pulse near the middle of each block of ~5000 pulses. As many as 30 such arrival times can be obtained in a single day's observing time, which is limited to about 2.5 hours by the tracking capability of the Arecibo telescope.

The least squares procedure for fitting the standard profiles to the individual 5 minute averages permits one to estimate uncertainties for the measured arrival times, and these estimates are listed for each observing system in Table 1. We show below that the estimates are in good agreement with the scatter of the postfit residuals from our timing model.

III. ANALYSIS OF THE DATA

a) The Timing Model

The observed pulse arrival times were fitted to the timing model of Blandford and Teukolsky (1976) and Epstein (1977, 1979), using a linearized least squares technique for parameter estimation. The model explicitly includes relativistic terms whose amplitudes vary periodically with orbital phase—gravitational redshift, transverse Doppler shift, post-Newtonian corrections to

the elliptical orbit, and gravitational propagation delay —as well as secular relativistic terms involving advance of periastron and orbital period change due to emission of gravitational radiation. The model is formulated on the assumption that general relativity is the "correct" theory of gravity, or at least has adequate accuracy for calculating the terms mentioned above; such accuracy is ensured, for all except the gravitational radiation term, by a number of high-precision tests within the solar system. In addition, it is assumed that the pulsar is intrinsically an accurate clock, and that the binary system consists of two stars that behave dynamically as point masses. The validity of these assumptions will be discussed in § III*b* and Appendix A.

In order to fit the measured pulse arrival times to the model, it is convenient to express the observed arrival times in terms of proper times T_p measured at the pulsar, so that the pulse phase ϕ can be calculated from a short Taylor series involving the pulsar rotation frequency $\nu = 1/P$ and its derivatives:

$$\phi(T_p) = \phi_0 + \nu T_p + \tfrac{1}{2}\dot{\nu} T_p^2 + \tfrac{1}{6}\ddot{\nu} T_p^3. \quad (1)$$

The conversion of observed arrival times to proper times was performed in two separate steps. First, the observed times were referred to the solar system barycenter (a relativistic correction for the annual variation in the rate of terrestrial clocks was included) and the interstellar plasma dispersion delay was removed, yielding "infinite frequency" barycentric arrival times. For these corrections, the position of the Earth was calculated by eighth-order interpolation of coordinates tabulated in the Lincoln Laboratory planetary ephemeris PEP 311, kindly supplied by I. I. Shapiro. Finally, the solar system barycentric arrival times were corrected to the pulsar frame by subtracting the variation in propagation time arising from the pulsar's orbital motion, including second-order relativistic terms and gravitational propagation delay in the vicinity of the companion (Taylor *et al.* 1976; Epstein 1977, 1979). The initial estimates of the parameters required for this procedure were taken from our earlier results (Taylor, Fowler, and McCulloch 1979).

Residuals (pulse phases from eq. [1], minus the nearest integer) were calculated for each of the measured pulse arrival times, and used in a least-squares fit for up to 20 quantities which fall into four broad categories: (1) traditional pulsar timing measurables right ascension α, declination δ, initial pulse phase ϕ_0, period P, and first and second derivatives $\dot{P}$, $\ddot{P}$ (Manchester and Peters 1972); (2) classically derivable elements of the binary orbit, including eccentricity e, projected semimajor axis of the pulsar orbit $a_p \sin i$, orbital period P_b, longitude of periastron ω_0, and time of periastron passage T_0; (3) relativistic terms, including the rate of advance of periastron passage $\dot{\omega}$, the variable part of the gravitational redshift and transverse Doppler shift γ, and the rate of change of the orbital period $\dot{P}_b$, representing the loss of orbital energy by gravitational radiation; and (4) up to six "instrumental offsets," required because some of the changes in observing technique implemented before March 1978 caused changes in the observed pulse profile (see Fig. 1), which in turn produce small, imperfectly calibrated delays in the pulse arrival time measurements. Each offset was an (initially unknown) constant added to every measured arrival time throughout the period that a given observing scheme was used.

In principle, one further parameter can be directly measured—the inclination angle i of the orbit plane with respect to the plane of the sky. This (relativistic) term is observable because of post-Newtonian departures from ellipticity and variations in gravitational propagation delay around the orbit (Epstein 1977). However, its amplitude is only ~ 30 μs, which makes it only marginally detectable in our highest quality data. Therefore, the inclination angle was not explicitly solved for in most of our arrival-time fits. It will be seen below, however, that under the assumption of a "clean" orbit, the angle i is derivable from other measurable quantities.

b) Parameter Estimation and Error Analysis

Least squares methods of extracting parameter estimates from observational data are very powerful, but if applied blindly can yield misleading results. In particular, standard procedures for estimating parameter uncertainties are based on ideal conditions in which measurement errors have a zero-mean, Gaussian distribution; real data conform to this ideal only approximately, at best. A cautious approach is also necessary when, as in this experiment, the available data are of nonuniform quality. For these reasons, we have made a number of tests to determine the magnitude of possible systematic biases, and to assess the effects of our assignment of relative weights to the several subsets of data.

A few sources of systematic errors in our data are well understood, but cannot be fully corrected retroactively. In this category are the small constant offsets in the pulse arrival times measured with some of the different observing systems described in Table 1. Unfortunately, no attempt was made during 1974–1977 to calibrate these offsets directly; instead, as mentioned in § III*a*, the offsets were determined empirically as part of the least squares fitting process. Errors in determining these offsets are expected to influence primarily those parameters which depend on slowly varying terms in the timing model—especially $\dot{P}$ and $\ddot{P}$. The offsets are not closely correlated with any of the orbital parameters. Another source of systematic errors is smearing of the observed pulse profiles, caused by imperfect ephemerides used to predict the apparent pulsar period for signal averaging purposes. These effects are most serious at

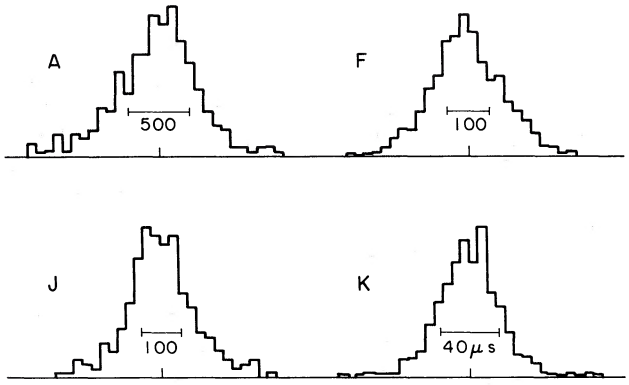

FIG. 2.—Histograms of the postfit residuals for timing measurements made with observing systems A, F, J, and K, each of which provided 300 or more pulse arrival times. The histograms have approximately Gaussian shapes; the half-widths are somewhat greater than the rms measurement uncertainties listed in Table 1, because the histograms do not reflect the reduced weights assigned to measurements taken at large zenith angles, with relatively poor signal-to-noise ratio.

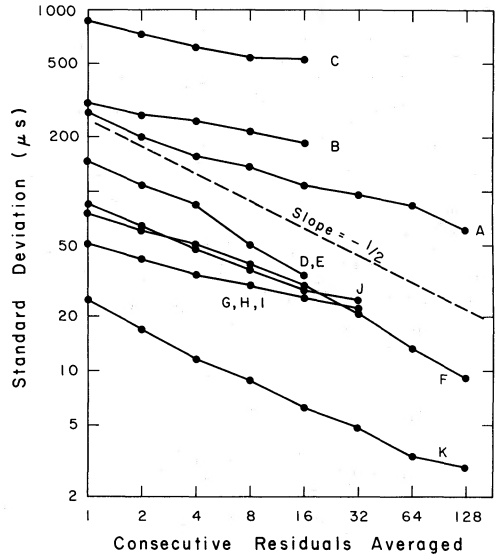

FIG. 3.—Standard deviations among averages of postfit residuals, obtained from sequences of consecutive measurements. If the measurements are uncorrelated, the standard deviations should decrease as $n^{-1/2}$, where n is the number of residuals averaged.

orbital phases when the period is changing rapidly, and can cause small but systematic biases in the fitted orbital parameters.

Much can be learned about the magnitude of hidden systematic effects in the data by careful inspection of postfit residuals from the least-squares solutions. Ideally the residuals should exhibit a zero-mean Gaussian distribution, and should show no correlations among adjacent values. In fact, we find that histograms of the residuals do show an approximately Gaussian shape, as illustrated in Figure 2. However, strings of consecutive residuals reveal some evidence of systematic errors, generally smaller than the Gaussian half-widths, in some of the data.

To estimate the magnitude of systematic errors in the observations, we averaged the postfit residuals from a global solution in groups of $n=2,4,8,\ldots$ consecutive values, computed standard deviations among the groups of each size for a given observing system, and plotted the results as shown in Figure 3. For uncorrelated residuals the standard deviations should diminish as $n^{-1/2}$. The most recently acquired data (obtained with system K) pass this test down to the 5 μs level or below, but at least some of the data taken during 1974–1976 are unreliable at the 100 μs level (system A) and at the 200 and 500 μs levels (systems B and C, respectively). Quite possibly, systems D, E, and F–J also contain nonrandom errors at the level of $\sim$30 μs.

Biases produced in parameter values by these systematic errors can be estimated by performing fits with different subsets of the data, or with different weighting schemes applied to the data. A sampling of such fits is presented in Table 2. The first solution is based on all of the available data, using the nominal weights listed in the last column of Table 1. These weights are roughly proportional to the inverse square of the total measurement uncertainty, including estimates of both random and systematic contributions. We regard this solution as our most objective fit to the data. The remaining solutions listed in Table 2 use much different weights, or omit some data entirely, or constrain certain parameters to fixed values. For each solution we list the fitted parameter values and their formal one-sigma errors. In general, the parameter estimates agree to within a few times the formal errors.

Our adopted values for the fitted parameters are listed at the bottom of Table 2, together with estimates of their overall uncertainties, which in a few cases are much larger than the formal errors. The error in celestial coordinates is dominated by an uncertainty of $\sim$0.″2 in the orientation of the planetary ephemeris coordinate system, relative to the FK4 system (I. I. Shapiro, private communication; see also Appendix A). The listed uncertainties in P, $\dot{P}$, and $\ddot{P}$ are dominated by possible bias from the uncalibrated offsets, in addition to possible intrinsic timing noise in the pulsar itself (Cordes and Helfand 1980). The uncertainties of $a_p \sin i$ and γ, which have the largest covariance (0.998) of any pair of parameters in the solution, have been set equal to 4 times the formal error. The remaining uncertainties are listed at 3 times the formal errors. In all cases, we believe that the listed uncertainties are realistic estimates of the combined effects of random and systematic errors.

The general goodness of fit of the adopted solution can be judged from Figure 4, which displays weighted

TABLE 2

PARAMETER ESTIMATES OBTAINED FROM LEAST-SQUARES FIT TO PULSE ARRIVAL TIMES[a]

Data Used	Right Ascension (1950.0)	Declination (1950.0)	P (s)	$\dot{P}$ (10^{-18})	$\ddot{P}$ (10^{-30} s^{-1})	$a_p \sin i$ (s)	e	P_b (s)	ω (deg)	T_0 (JED−2440000)	$\dot{\omega}$ (deg/yr)	γ (s)	P_b (10^{-12})
1974 Sep–1981 Mar (nominal weights)	$19^h13^m12\overset{s}{.}4685$	16°01′08″.163	0.0590299952709	8.628	−58	2.34186	0.617139	27906.98161	178.8656	2321.4332092	4.2261	0.00438	−2.30
	1	1	2	2	13	6	2	1	5	5	2	6	7
1974 Sep–1981 Mar (P2=0.0)	19 13 12.4685	16 01 08.172	0.0590299952715	8.6189	0[†]	2.34186	0.617140	27906.98160	178.8660	2321.4332095	4.2260	0.00438	−2.21
	1	1	1	2		7	2	6	6	6	2	6	8
1974 Sep–1981 Mar (systems B, C omitted) ...	19 13 12.4685	16 01 08.162	0.0590299952705	8.634	−96	2.34183	0.617139	27906.98162	178.8657	2321.4332090	4.2261	0.00436	−2.35
	1	2	2	3	19	7	2	1	6	5	2	6	8
1974 Sep–1981 Mar (uniform weights)	19 13 12.4690	16 01 08.180	0.0590299952714	8.623	−33	2.34198	0.617136	27906.98158	178.8666	2321.4332104	4.2247	0.00450	−2.16
	4	10	2	3	28	31	9	3	15	13	7	30	28
1976 Dec–1981 Mar (A, B, C omitted)	19 13 12.4686	16 01 08.159	0.0590299952720	8.630	−142	2.34183	0.617139	27906.98160	178.8658	2321.4332095	4.2261	0.00435	−2.16
	1	2	2	3	36	10	2	3	6	6	3	9	25
1978 June–1981 Feb (System F only)	19 13 12.4687	16 01 08.165	0.0590299952713	8.644	−580	2.34216	0.617133	27906.98157	178.8645	2321.4332099	4.2243	0.00464	−2.38[b]
	2	4	2	4	90	32	3	3	20	5	9	27	
1981 Feb–Mar only	19 13 12.4685[b]	16 01 08.171[b]	0.0490299952714	8.618[b]	0[b]	2.34186	0.617134	27906.98185	178.8659	2321.4332097	4.2261[b]	0.00438[b]	−2.38[b]
			2			3	13	31	4	2			
Adopted values	19 13 12.4685	16 01 08.163	0.0590299952709	8.628	−58	2.34186	0.617139	27906.98161	178.8656	2321.4332092	4.2261	0.00438	−2.30
	130	200	20	20	1200	24	5	3	15	15	7	24	22

[a]For all solutions except number 4, the data included in the fit were assigned weights as listed in the last column of Table 1. Formal one-sigma errors, listed immediately below each parameter value, are known to be underestimates of the true uncertainties. However, the uncertainties quoted beneath the "adopted" values include estimates of possible systematic errors, and are thought to be conservative. Some details of the error estimation process are given in § III.

[b]These parameters were held fixed at the quoted value.

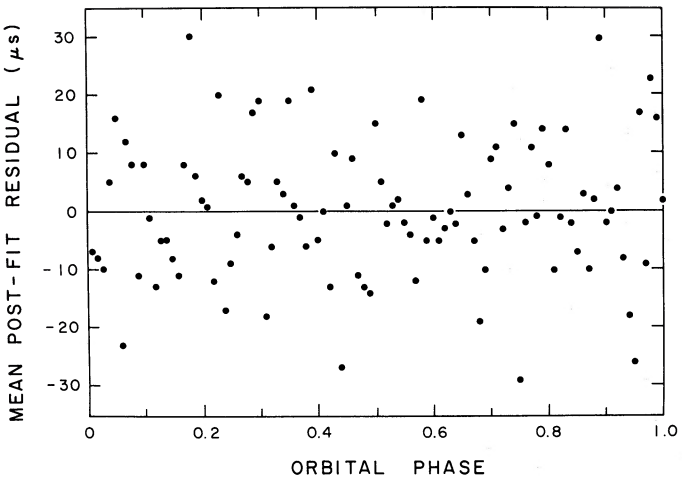

FIG. 4.—Weighted averages of the postfit timing residuals, plotted in 100 equally spaced bins of orbit phase. Each point corresponds to about 25 individual measurements of pulse arrival time.

means of the postfit residuals from the first solution in Table 2, averaged into 100 equally spaced bins of orbital phase. It is evident that there are no systematic phase-dependent trends exceeding about 20 μs, and that the Blandford-Teukolsky-Epstein model proves a very good description of the observed pulse arrival times.

IV. COMPONENT MASSES AND SIZE OF THE ORBIT

Only seven quantities are required to determine completely (up to rotations about the line of sight) the orbital parameters and the masses of the two stars. For this purpose, we choose the five classically measurable orbital elements $a_p \sin i$, e, P_b, T_0, ω_0, and the observable relativistic quantities $\dot{\omega}$ and γ. The expected values of $\dot{\omega}$ and γ can be expressed in terms of the classical parameters and the masses of the pulsar and its companion, m_p and m_c, as follows:

$$\dot{\omega}=3G^{2/3}c^{-2}(P_b/2\pi)^{-5/3}(1-e)^{-1}(m_p+m_c)^{2/3}$$

$$=2.11353\left(\frac{m_p+m_c}{M_\odot}\right)^{2/3}\ \text{deg yr}^{-1}, \qquad (2)$$

$$\gamma=G^{2/3}c^{-2}e(P_b/2\pi)^{1/3}m_c(m_p+2m_c)(m_p+m_c)^{-4/3}$$

$$=0.00293696\left(\frac{m_c}{M_\odot}\right)\left(\frac{m_p+2m_c}{M_\odot}\right)\left(\frac{m_p+m_c}{M_\odot}\right)^{-4/3}\ \text{s}, \qquad (3)$$

where in the second line of each expression we have inserted the adopted values of the well-determined orbited elements, and the constants $G=6.6732\times10^{-8}$ dyn cm^2 g^{-2}, $c=2.997925\times10^{10}$ cm s^{-1}, and $M_\odot=1.989\times10^{33}$ g.

By inserting the measured values of $\dot{\omega}$ and γ in equations (2) and (3), one can solve simultaneously for the masses of the pulsar and its companion. The results are $M=m_p+m_c=2.8275\pm0.0007\ M_\odot$, $m_p=1.42\pm0.06\ M_\odot$, and $m_c=1.41\pm0.06\ M_\odot$. It is interesting to note, in passing, that PSR 1913+16 is the only radio frequency pulsar whose mass has been measured, and that this determination marks the first use of general relativity as a tool for high-precision astrophysical measurement.

Given the masses of the two stars, plus the classically derived orbital elements, all remaining unknown orbital parameters—the inclination i, and the semimajor axes of the relative orbit, pulsar orbit, and companion orbit a, a_p, a_c—may be calculated from known quantities using the relations

$$\sin i=G^{-1/3}c(a_p \sin i/m_c)(P_b/2\pi)^{-2/3}\times(m_p+m_c)^{2/3}, \qquad (4)$$

$$a=G^{1/3}c^{-1}(P_b/2\pi)^{2/3}(m_p+m_c)^{1/3}, \qquad (5)$$

$$a_p=am_c(m_p+m_c)^{-1}, \qquad (6)$$

$$a_c=am_p(m_p+m_c)^{-1}. \qquad (7)$$

The resulting values are listed together with the mass determinations, in Table 3.

V. GRAVITATIONAL RADIATION

a) *Observed Decay of the Orbit*

The most far-reaching result of this experiment is our measurement of a secular decrease of orbital period,

TABLE 3

QUANTITIES DERIVED FROM THE ORBITAL PARAMETERS

Total mass	$M=2.8275\pm0.0007\ M_\odot$
Pulsar mass	$m_p=1.42\pm0.06\ M_\odot$
Companion mass	$m_c=1.41\pm0.06\ M_\odot$
Inclination	$\sin i=0.72\pm0.03$
Relative semimajor axis	$a=6.5011\pm0.0005$ lt-sec
Pulsar semimajor axis	$a_p=3.24\pm0.13$ lt-sec
Companion semimajor axis	$a_c=3.26\pm0.13$ lt-sec

consistent with the loss of energy through emission of quadrupole gravitational radiation, as predicted by general relativity. As pointed out by Wagoner (1975) and Esposito and Harrison (1975), the expected decrease of orbital period can be calculated from the results of Peters and Mathews (1963). A convenient form of the relevant expression is

$$\dot{P}_b=-\frac{192\pi G^{5/3}}{5c^5}(P_b/2\pi)^{-5/3}(1-e^2)^{-7/2}\times\left(1+\frac{73}{24}e^2+\frac{37}{96}e^4\right)m_p m_c(m_p+m_c)^{-1/3}. \quad (8)$$

By inserting the measured values of P_b, e, m_p, and m_c from Tables 2 and 3, one obtains the prediction $\dot{P}_b=(-2.403\pm0.005)\times10^{-12}$, in excellent agreement with the observed value $(-2.30\pm0.22)\times10^{-12}$. A striking illustration of the self-consistency among the measured values of $\dot{\omega}$, γ, and $\dot{P}_b$ is contained in Figure 5. Within a small region of the mass-mass plane—namely, the thickened portion of the line passing through the cross-hatched region in the figure — the measured effects involving periastron advance, gravitational redshift/transverse Doppler shift, and gravitational radiation are all consistent with a single solution for the masses. This agreement provides powerful support for the validity of the model, and suggests strongly that any nonrelativistic contributions to the three parameters $\dot{\omega}$, γ, and $\dot{P}_b$ are small. Similarly, these results imply that any errors (see Ehlers *et al.* 1976; Rosenblum 1978; Walker and Will 1980) in the general relativistic calculation of $\dot{P}_b$ are small or nonexistent.

The most reliable estimate of the value of $\dot{P}_b$ (and its uncertainty) comes from the global solution for all of the system parameters, as discussed in § III*b*. However, a pictorial representation of the observed change of orbital period is also instructive. To provide such an illustration, we divided the pulse arrival time data into 14 blocks, each of which consists of observations made near a given epoch. Within each block, a least squares estimate was made of a time of periastron passage close to the nominal block center. These periastron times are listed, together with their estimated uncertainties, in Table 4. If the orbital period had remained constant,

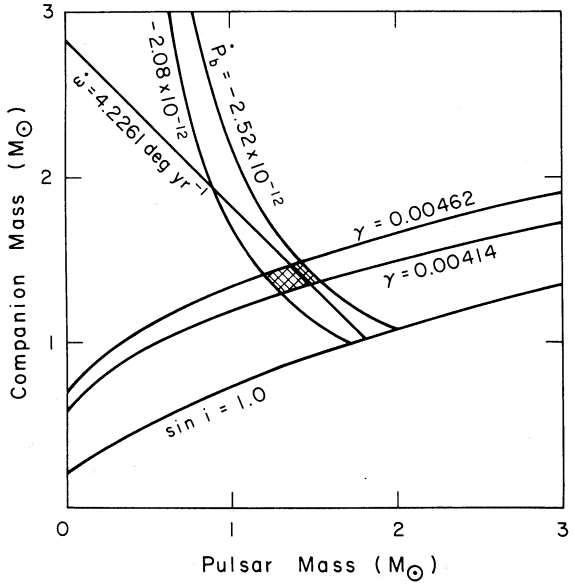

FIG. 5.—Curves delimiting allowed combinations of pulsar mass and companion mass. The portion of the plane below $\sin i=1.0$ is forbidden by the observed mass function, and the remaining curves correspond to eqs. (2), (3), and (8). The measured values of $\dot{\omega}$, γ, and $\dot{P}_b$ are consistent with a mass solution on the thickened portion of the sloping straight line.

one would expect the periastron times to be separated by integral multiples of P_b. Orbit phase residuals, i.e., departures from integral multiples, which increase (or decrease) linearly with time would indicate an error in the assumed value of P_b. On the other hand, a parabolic trend in the orbit phase residuals is indicative of a constantly changing period. The observed behavior, illustrated in Figure 6, shows the expected parabolic shape. The average slope and intercept of the parabola have been adjusted for best fit to the data, and agree

TABLE 4

OBSERVED TIMES OF PERIASTRON PASSAGE

Approximate Date	Periastron Passage (JED−2,440,000)
1974.77	2331.4461316±0.0000008
1974.93	2389.5856753±0.0000007
1976.13	2826.9242544±0.0000024
1976.93	3118.5909684±0.0000006
1977.58	3356.6401037±0.0000005
1977.96	3493.5910317±0.0000003
1978.23	3593.3972490±0.0000003
1978.42	3663.4877010±0.0000007
1978.82	3807.5445713±0.0000005
1979.31	3988.4231536±0.0000003
1980.10	4276.5368958±0.0000003
1980.59	4454.5085004±0.0000009
1980.59	4455.4774930±0.0000003
1981.14	4656.3819172±0.0000002

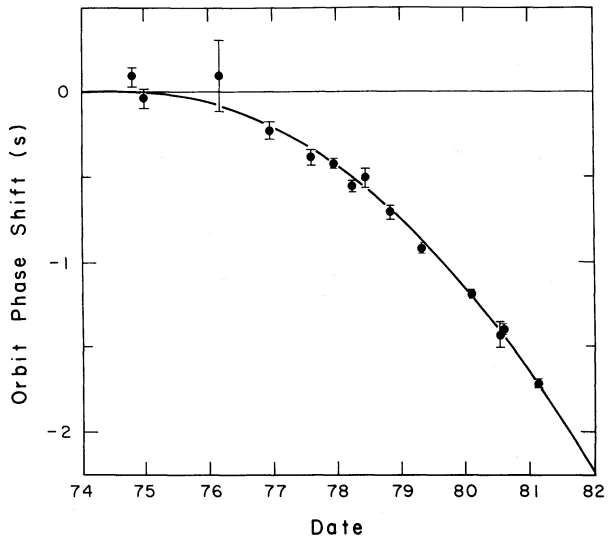

FIG. 6.—Orbital phase residuals, obtained from the data listed in Table 4. If the orbital period had remained constant, the points would be expected to lie on a straight line. The curvature of the parabola drawn through the points corresponds to the general relativistic prediction for loss of energy to gravitational radiation, or $\dot{P}_b = -2.40 \times 10^{-12}$.

well with the adopted values of P_b and T_0 listed in Table 2. The curvature of the parabola corresponds to the predicted value $P_b = -2.40 \times 10^{-12}$ (cf. eq. [8]). It is clear that the observations of orbit phase are in excellent agreement with the predicted loss of energy by gravitational radiation.

b) *Other Theories of Gravity*

A number of other tentatively viable theories of gravitation also predict the emission of gravitational waves, and it is useful to compare their predictions with our observations. Will (1977) has parametrized a number of theories in a form facilitating specific predictions of the magnitude of binary orbital period changes due to gravitational radiation. We have integrated Will's expressions around an orbit to provide a general expression for the time-averaged binary period change due to emission of gravitational waves, obtaining the expression (Weisberg and Taylor 1981)

$$\dot{P}_b = -\frac{16\pi G^{5/3}}{5c^5}(P_b/2\pi)^{-5/3}(1-e)^{-7/2} \times \left[(\kappa_1-\kappa_2)\left(1+\frac{7}{2}e^2+\frac{1}{2}e^4\right) + \kappa_2\left(1+3e^2+\frac{3}{8}e^4\right)\right] m_p m_c (m_p+m_c)^{-1/3} - \frac{4\pi^2 G}{c^3}\xi \mathcal{G}^2 P_b^{-1}\left(1+\frac{1}{2}e^2\right) \times (1-e^2)^{-5/2} m_p m_c (m_p+m_c)^{-1}, \quad (9)$$

where $\mathcal{G}$ is the difference in self-gravitational binding energy per unit mass in the pulsar and companion, and κ_1, κ_2, and ξ are fixed parameters in each theory of gravitation. The first term in equation (9) can be identified as the Peters-Mathews (PM) term, which represents the analog of general-relativistic quadrupole radiation in each theory (plus "electric monopole" and "magnetic quadrupole" contributions in some theories). The final term is the dipole radiation term. The dipole term is identically zero in general relativity, but in other theories its magnitude is much greater than the PM term unless the pulsar and its companion are virtually identical (i.e., unless $\mathcal{G}^2 \to 0$). The calculated values of the PM term, the dipole term, and the total $\dot{P}_b$ are shown for each theory of gravity in Table 5, along with the values of κ_1, κ_2, and ξ given by Will. For these calculations we used the values of m_p and m_c listed in Table 3, which are based on general relativity. The correct values of m_p and m_c would be somewhat different if calculated consistently in other gravitational theories (cf. Eardley 1975; Will 1980), but this fact does not alter the following important conclusion: *With the exception of general relativity and the Brans-Dicke theory, none of the theories predicts even the proper sign of orbital period change due to emission of gravitational radiation, let alone the proper magnitude.* We stress that this conclusion is valid regardless of the magnitude of the dipole term; i.e., regardless of the relative masses of the two orbiting components. Furthermore, even the Brans-Dicke theory predicts a magnitude of $\dot{P}_b$ much larger than observed, unless either the coupling constant ω approaches infinity (in which case all predictions of the theory reduce to those of general relativity), or unless the internal structure of the two stars is so nearly identical[2] that $\mathcal{G}^2 \lesssim 10^{-4}$.

Thus, our observations of the binary pulsar's orbital period decrease seem to rule out a number of theories of gravitation previously considered viable. Of the two remaining well-studied theories—general relativity and the Brans-Dicke theory—only general relativity predicts an orbital period decrease very close to the observed value without invoking additional ad hoc hypotheses. The observed $\dot{P}_b$, a measurable manifestation of the emission of gravitational waves, provides compelling evidence for the existence of such waves, and perhaps the deepest test of the validity of general relativity to date.

We are deeply indebted to our colleagues R. A. Hulse, L. A. Fowler, and P. M. McCulloch, each of whom made important contributions to earlier phases of this project. We also thank J. M. Cordes, G. E. Gullahorn, and J. M. Rankin, who assisted with or provided much

[2] Our data on the masses are, of course, not inconsistent with $\mathcal{G}=0$.

TABLE 5

PREDICTED RATE OF ORBITAL PERIOD CHANGE, ACCORDING TO VARIOUS THEORIES OF GRAVITY

Theory	κ_1[a]	κ_2[a]	$\dot{P}_b$ (quadrupole)[b] (10^{-12})	Dipole Parameter, ξ	$\dot{P}_b$ (dipole) (10^{-12})	$\dot{P}_b$ (total) (10^{-12})
General relativity	12	11	-2.40	0	0	-2.40
Brans-Dicke	$12-\frac{5}{2+\omega}$	$11-\frac{11.25}{2+\omega}$	$-2.40+\frac{0.876}{2+\omega}$	$\frac{2}{2+\omega}$	$\frac{-3.89\times10^4\,\mathcal{G}^2}{2+\omega}$	$-2.40+\frac{0.876-3.89\times10^4\mathcal{G}^2}{2+\omega}$
Rosen	$-\frac{21}{2}$	$-\frac{23}{2}$	$+2.07$	$-\frac{20}{3}$	$1.30\times10^5\mathcal{G}^2$	$\geq+2.07$
Ni	-18	-19	$+3.56$	$-\frac{400}{3}$	$2.59\times10^6\mathcal{G}^2$	$\geq+3.56$
Lightman-Lee	$-\frac{21}{2}$	$\frac{73}{8}$	$+2.46$	$-\frac{125}{3}$	$8.10\times10^5\mathcal{G}^2$	$\geq+2.46$
Observed	...	...	...	...	...	-2.30 ± 0.22

[a] PM parameter.

[b] In some theories the Peters-Mathews ("quadrupole") term also includes a monopole contribution (Will 1977).

of the data taken during 1975–1976. The staff of the Arecibo Observatory has been helpful and cooperative throughout the 6 years of data taking. We acknowledge financial support from the National Science Foundation. This paper is contribution number 475 of the Five College Observatories.

APPENDIX A

THE NATURE OF THE COMPANION STAR

Our primary concern here is to investigate whether both stars act dynamically as point masses. If they do not, then various tidal and rotational effects will complicate our relativistic analysis of the data. For example, tidal or rotational deformation of either star could cause a secular advance of periastron indistinguishable from the expected relativistic effect. Similarly, viscous dissipation of orbital energy in either stellar component could result in an orbital period change that would mask an orbital period decrease due to emission of gravitational radiation.

The rate of tidally or rotationally induced periastron advance is proportional to R_*^5, while the viscous orbital decay term is proportional to R_*^9, where R_* is the stellar radius. Consequently, both terms are utterly negligible for the pulsar (Smarr and Blandford 1976). However, such effects may be important in the companion if it is not also a collapsed star. Thus, we must investigate the nature of the companion.

It is clear that the companion cannot be a main-sequence star. The absence of eclipses of the pulsar strongly constrains the size of the companion (Hulse and Taylor 1975*a*); moreover, tidal deformation of a main-sequence star would result in a periastron advance much larger than the observed value (Masters and Roberts 1975). The only remaining viable candidates for the companion are a helium star, white dwarf, neutron star, or black hole. The latter two are sufficiently compact that they, like the pulsar, would act dynamically as point masses. However, a helium star or a white dwarf may not act as a point mass. Smarr and Blandford (1976) show that the quadrupole moment of a tidally deformed helium star or a rapidly rotating white dwarf is sufficient to induce periastron advance with a magnitude as large as the expected relativistic effect. It is also possible that viscous dissipation of orbital energy in a deformed white dwarf or helium star could cause an orbital period change of the same magnitude as the expected period decrease caused by gravitational radiation. At present, however, lack of understanding of the sources of stellar viscosity precludes an accurate calculation of the importance of this effect, and estimates vary by orders of magnitude. Ionic, electronic, and molecular viscosity will cause negligible orbital decay, but possible magnetic or turbulent viscosity might induce an orbital period derivative up to several orders of magnitude larger than the expected relativistic value (Balbus and Brecher 1976; Will 1976; Smarr and Blandford 1976). Considering the present large uncertainties in the magnitude of possible viscous losses in white dwarf or helium stars, we consider it very unlikely that they would fortuitously be of just the same magnitude as expressed losses due to gravitational radiation.

Clearly it is of great interest to determine the nature of the companion, so that the importance of nonrelativistic effects can be assessed. Both experimental and

theoretical investigations have been carried out. An upper limit of 60 μJy has been placed on the companion's pulsed emission at 430 MHz (Taylor *et al.* 1976). Of course, the companion could still be a pulsar whose beamed emission does not intersect the Earth. Optical studies have revealed a star with $m_V=22.5$, $m_R=20.9$, very near the position of the pulsar (Kristian and Westphal 1978; Crane, Nelson, and Tyson 1979). The object's optical pulsations, if any, are fainter than a time-averaged magnitude $m_R=26.5$ (Elliott *et al.* 1980).

Although Crane *et al.* consider it likely that the visible object is a helium star orbiting the pulsar (a white dwarf would not be visible at the system's estimated distance of 5 kpc), at present the only evidence in favor of a physical association is the positional coincidence. Elliott *et al.* (1980) have done the most thorough astrometry of the PSR 1913+16 field, and give a position for the candidate star of R.A. $19^h13^m12^s.455\pm0^s.007$, decl. $16°01'08''.50\pm0''.09$, at epoch 1978.6, mean equator and equinox 1950.0, in the FK4 system. If we translate our pulsar position to the FK4 system by allowing for the *E*-terms of aberration (see Elliott *et al.* 1980), and combine the optical and radio position uncertainties quadratically, we find that the candidate star lies $0''.13\pm0''.21$ east of the pulsar, and $0''.36\pm0''.22$ north of it. The discrepancy in declination is not large enough to reject convincingly the association hypothesis. Conclusive evidence on the nature of the candidate star will require further information, such as an optical spectrum showing (or lacking) the features expected for a helium star, and the periodic Doppler shifts expected from the companion's orbital motion.

A helium star companion would probably have a strong, radiation driven stellar wind (Smarr and Blandford 1976). A search for variations in the pulsar's dispersion measure with respect to orbit phase has yielded an upper limit of 0.002 pc cm^{-3}, which leads to an upper limit on the mean electron density inside the pulsar's orbit of about 10^5 cm^{-3}. This limit severely restricts the possible stellar wind parameters (i.e., $\dot{m}/v<10^{-17}\ M_\odot\ \mathrm{yr}^{-1}/\mathrm{km\ s}^{-1}$) and suggests that the companion is not a helium star. It is possible, however, that dispersion variations are not present because the pulsar radiation is sweeping the ionized gas from the system, or because the stellar wind is much weaker than expected.

Theoretical investigations of the nature of the companion have focused on construction of evolutionary scenarios plausibly leading to the present orbital configuration. The most likely evolutionary path leads to a companion that is a neutron star or perhaps a black hole (Flannery and van den Heuvel 1975; de Loore, De Grève, and De Cuyper 1975; Webbink 1975; Smarr and Blandford 1976; Srinivasan and van den Heuvel 1981). The preference for a neutron star companion is further strengthened by our determination that m_c is very close to the Chandrasekhar limit; it is plausible that all neutron stars have approximately this mass, because they form when the core of an evolving star becomes so massive that it can no longer be supported by electron degeneracy pressure.

According to the favored model, the system originally consisted of a pair of main-sequence stars with total mass of 20–30 $M_\odot$, orbiting each other with a several-day period. The more massive star overflowed its Roche lobe and lost much of its mass to the secondary, leaving a helium core. The core eventually exploded as a supernova, thereby creating a neutron star. The system then underwent a massive X-ray binary stage as the stellar wind from the secondary accreted onto the neutron star. The secondary's envelope finally expanded and engulfed the neutron star, creating a double-core binary (Taam, Bodenheimer, and Ostriker 1978; Delgado 1980). The neutron star then rapidly spiraled deep inside the common envelope until frictional luminosity was so great as to drive away the envelope, leaving a neutron star in a circular orbit around a helium star. (According to Taam 1979, large initial orbital separations are necessary to prevent subsequent merging of the two cores.) Alternatively, if the secondary did not expand sufficiently to create a double-core binary, it would still overflow its Roche lobe, and the ensuing mass loss would also result in a very short period binary consisting of a helium star and a collapsed star in mutual circular orbits. The helium core of the secondary finally finished its evolution as a supernova, nearly disrupting the system as shown by its present high eccentricity, and leaving a second neutron star. In this scenario, the observable pulsar is apparently the older neutron star, as indicated by its weak magnetic field, and its short pulse period is the result of its having been spun up during its accretion phase (Smarr and Blandford 1976; Srinivasan and van den Heuvel 1981). Slight variations of the above scenario permit the creation of a black hole companion, either as the result of a more massive supernova precursor or as the result of accretion onto the first neutron star. Alternative evolutionary sequences can be constructed that lead to a degenerate dwarf or a helium star companion in the present system, but only with difficulty (Smarr and Blandford 1976; Blandford and DeCampli 1981). One of the main problems with such alternate sequences is the difficulty of explaining the present tight orbit. *Any* scenario must include a mechanism for shrinking the orbit greatly, since the progenitor stars themselves at some stage(s) of their lives were almost certainly larger than the present orbit. The shrinkage is naturally accomplished during either the secondary's mass-loss phase or the double-core phase in models leading to a neutron star or black hole companion, but it is difficult to devise a mechanism creating the present small but eccentric orbit if the companion is now a degenerate dwarf or helium star.

In summary, we may state that, although the evidence is not yet as conclusive as might be wished, available data and theoretical considerations indicate that the companion of PSR 1913+16 is probably a neutron star or black hole—either of which can be treated dynamically as a point mass.

APPENDIX B

ADDITIONAL OBSERVATIONAL DATA

a) Profile Changes and Polarization Measurements

According to general relativity, if the pulsar spin and orbital angular velocities are not aligned, geodetic precession should cause the spin axis to precess with a period of about 300 yr (Barker and O'Connell 1975; Esposito and Harrison 1975; Hari-Dass and Radhakrishnan 1975). As a consequence, the angle between the spin axis and the line of sight would change at a rate $\sim 1^\circ\ \mathrm{yr}^{-1}$, and the observed pulse profile would be expected to change significantly. Our observations taken with observing system F (Table 1) constitute a uniform set of observed pulse profiles spanning more than 2 years, and we find no measurable changes in pulse shape within these data. An earlier tentative report of profile change (McCulloch, Taylor, and Weisberg 1979; Taylor, Fowler, and McCulloch 1979) is now known to be the result of a small degree of circular polarization which changes sign near the center of the pulse profile, as shown in Figure 7. Barring some fortuitous geometry, the lack of observed profile change indicates either that the pulsar beam is much wider in latitude than in longitude, or that the pulsar spin axis is very nearly perpendicular to the orbital plane.

If, as seems likely, alignment of angular momenta is the correct explanation for the lack of observable precession, then the data on PSR 1913+16 furnish some evidence concerning the emission mechanism of pulsars (Taylor 1981). Our data indicate that the orbital plane is inclined by about 45° to the plane of the sky; consequently, if the spin axis is perpendicular to the orbital plane, the observed radio emission must radiate from a pulsar latitude of about 45°. This geometry is fully consistent with polar cap emission models, but not with those involving relativistic beaming at the velocity-of-light cylinder, which must be in the direction of the equatorial plane.

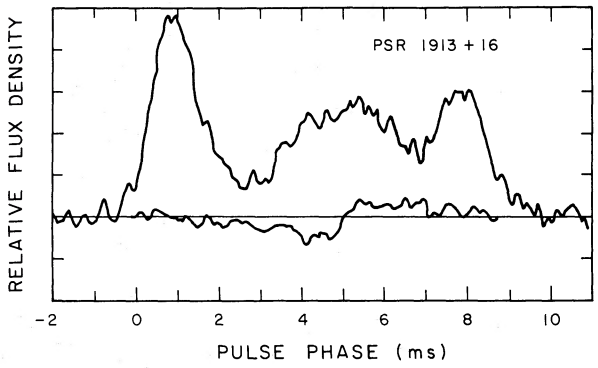

FIG. 7.—Stokes parameters I (total intensity, *upper curve*) and V (circular polarization, *lower curve*) for the integrated profile of PSR 1913+16 at 430 MHz.

b) Dispersion Measure

The dispersion measure (DM) of PSR 1913+16 was measured by Hulse and Taylor (1975*a*), who give the value $\mathrm{DM} = 167 \pm 5\ \mathrm{cm}^{-3}$ pc based on measurements made at 426 and 434 MHz. Pulse arrival time measurements made at 430 and 1410 MHz during 1976–1977 (observing systems D, E, G, and H in Table 1) were found to be consistent with the value $\mathrm{DM} = 171.64 \pm 0.01\ \mathrm{cm}^{-3}$ pc, which was quoted by Fowler (1979) and was used for dispersion compensation in all observations made during 1976–1980. This value corresponds to a dispersive delay of 59.183 pulse periods between 1410 and 430 MHz. More complete dispersion measurements made in 1981 February at frequencies of 430, 433, 1396, and 1404 MHz yield a dispersion of $168.77 \pm 0.01\ \mathrm{cm}^{-3}$ pc, which corresponds to a 1410-to-430 MHz delay of 58.193 ± 0.003 periods. We conclude that the dispersion measure used in our earlier observations was in error, owing to a miscount by exactly one period in the delay. The only significant effect of this error on our data is that the pulse profiles obtained with observing system F (prior to 1981 February) are spuriously broadened by an additional $\sim 450\ \mu$s. The effect on analysis of the timing data is negligible.

REFERENCES

Balbus, S. A., and Brecher, K. 1976, *Ap. J. (Letters)*, **203**, 202.
Barker, B. M., and O'Connell, R. R. 1975, *Ap. J. (Letters)*, **199**, L25.
Blandford, R. D., and DeCampli, W. M. 1981, in *IAU Symposium 95, Pulsars*, ed. R. Wielebinski and W. Sieber (Dordrecht: Reidel), in press.
Blandford, R. D., and Teukolsky, S. A. 1976, *Ap. J.*, **205**, 580.
Boriakoff, V. 1973, Ph.D. thesis, Cornell University.
Cordes, J. M., and Helfand, D. J. 1980, *Ap. J.*, **239**, 640.
Crane, P., Nelson, J. E., and Tyson, J. A. 1979, *Nature*, **280**, 367.
de Loore, C., De Grève, J. P., and De Cuyper, J. P. 1975, *Ap. Space Sci.*, **36**, 219.

Delgado, A. J. 1980, *Astr. Ap.*, **87**, 343.
Eardley, D. M. 1975, *Ap. J.* (*Letters*), **196**, L59.
Ehlers, J., Rosenblum, A., Goldberg, J. N., and Havas, P. 1976, *Ap. J.* (*Letters*), **208**, L77.
Elliott, K. H., Peterson, B. A., Wallace, P. T., Jones, D. H. P., Clements, E. D., Hartley, K. F., and Manchester, R. N. 1980, *M.N.R.A.S.*, **192**, 51P.
Epstein, R. 1977, *Ap. J.*, **216**, 92.
_____. 1979, *Ap. J.*, **231**, 644.
Esposito, L. W., and Harrison, E. R. 1975, *Ap. J.* (*Letters*), **196**, L1.
Flannery, B. P., and van den Heuvel, E. P. J. 1975, *Astr. Ap.*, **39**, 61.
Fowler, L. A. 1979, Ph.D. thesis, University of Massachusetts.
Fowler, L. A., Cordes, J. M., and Taylor, J. H. 1979, *Australian J. Phys.*, **32**, 35.
Gullahorn, G. E., and Rankin, J. M. 1978, *A.J.*, **83**, 1219.
Hari-Dass, N. D., and Radhakrishnan, V. 1975, *Ap. Letters*, **16**, 135.
Hulse, R. A. 1975, Ph.D. thesis, University of Massachusetts.
Hulse, R. A., and Taylor, J. H. 1974, *Ap. J.* (*Letters*), **191**, L59.
_____. 1975*a*, *Ap. J.* (*Letters*), **195**, L51.
_____. 1975*b*, *Ap. J.* (*Letters*), **201**, L55.
Kristian, J., and Westphal, J. A. 1978, *IAU Circ.*, No. 3242.
Manchester, R. N., and Peters, W. L. 1972, *Ap. J.*, **173**, 221.
Masters, A. R., and Roberts, D. H. 1975, *Ap. J.* (*Letters*), **195**, L107.
McCulloch, P. M., Taylor, J. H., and Weisberg, J. M. 1979, *Ap. J.* (*Letters*), **227**, L133.
Peters, P. C., and Mathews, J. 1963, *Phys. Rev.*, **131**, 435 (PM).
Rosenblum, A. 1978, *Phys. Rev. Letters*, **41**, 1003.
Smarr, L. L., and Blandford, R. 1976, *Ap. J.*, **207**, 574.
Srinivasan, G., and van den Heuvel, E. P. J. 1981, *Astr. Ap.*, in press.
Taam, R. E. 1979, *Ap. Letters*, **20**, 29.
Taam, R. E., Bodenheimer, P., and Ostriker, J. P. 1978, *Ap. J.*, **222**, 269.
Taylor, J. H. 1981, in *IAU Symposium 95, Pulsars*, ed. R. Wielebinski and W. Sieber (Dordrecht: Reidel), in press.
Taylor, J. H., Fowler, L. A., and McCulloch, P. M. 1979, *Nature*, **277**, 437.
Taylor, J. H., and Huguenin, G. R. 1971, *Ap. J.*, **167**, 273.
Taylor, J. H., Hulse, R. A., Fowler, L. A., Gullahorn, G. E., and Rankin, J. M. 1976, *Ap. J.* (*Letters*), **206**, L53.
Wagoner, R. 1975, *Ap. J.* (*Letters*), **196**, L63.
Walker, C., and Will, C. M. 1980, *Ap. J.* (*Letters*), **242**, L129.
Webbink, R. F. 1975, *Astr. Ap.*, **41**, 1.
Weisberg, J. M., and Taylor, J. H. 1981, *Gen. Rel. Grav.*, in press.
Will, C. M. 1976, *Ap. J.*, **205**, 861.
_____. 1977, *Ap. J.*, **214**, 826.
_____. 1980, *Ann. NY Acad. Sci.*, **336**, 307.

JOSEPH H. TAYLOR and JOEL M. WEISBERG: Joseph Henry Laboratories, Department of Physics, Princeton University, Princeton, NJ 08544